PERFORMANCE ANALYSIS OF A VARIABLE BARRIER ENERGY TRANSFER SCREW

Todd A. Hogan, Mark A. Spalding, and Eung Kyu Kim, The Dow Chemical Company, Midland, MI
Robert A. Barr and Jeff A. Myers, BARR Inc., Virginia Beach, VA

Abstract

High plastication rates and high quality extrudates are often difficult to produce using single-screw extruders, especially at low discharge temperatures. A new screw called a variable barrier energy transfer (VBET) screw was recently developed to plasticate at high rates, low discharge temperatures, and with high melt qualities. The fundamental operation of the screw along with performance aspects will be presented. A comparison is made between the melting, pumping, and mixing characteristics of an Energy Transfer (ET) screw and VBET screw.

Introduction

It is well known that a polymer fed to a single-screw, plasticating extruder is first compacted into a solid bed, and then the solid bed, rotating with the screw, melts (or devitrifies) by rubbing on the hot barrel (1). A thin melt film is formed between the solid bed and the barrel, and melting of the solid bed occurs primarily by the energy dissipated in the melt film. This melting mechanism is called dissipative melting. When a conventional single flighted screw is used during extrusion operations, most of the mixing also occurs during this melting process.

As processors drive toward higher plastication rates while maintaining high quality extrudates, limitations are reached in the ability to effectively melt and mix using single-screw extruders. Usually higher rates are achieved by increasing the screw speed of the extruder. However, high screw speeds can transport solids close to the screw tip, which can decrease extrudate quality. Single-screw extruders equipped with specialized mixing sections can trap and melt these solids to improve extrudate quality. This is due to the complex flow paths and added opportunities for shear-induced mix-melting provided by mixing sections, but the addition of mixing sections can sometimes decrease rate and increase extrudate temperatures.

There have been numerous experimental studies of melting, flow, and mixing in single-screw extruders. To visualize screw performance, Maddock conducted solidification experiments, where he halted screw rotation, simultaneously cooled the barrel, and then pushed out the screw (2). With this technique, Maddock demonstrated that melting and mixing in a conventional screw were improved by reducing the screw-channel depths, increasing the discharge pressure, or cooling the screw root. However, each of these adjustments had the unwanted consequence of reducing the rate. Later, he found that extrudate quality could be improved with the addition of a fluted or Maddock mixing section on the downstream end of the screw (3). This mixer trapped and melted any solid material transported close to the screw tip and caused the extrudate temperature to increase.

Another approach to overcome melting and mixing limitations has been the development of solid/melt mixing screws. There are two different solid/melt mixing screws commercially available, the Wave Screw (4, 5) and the Barr Energy Transfer (ET) screw (6-10). Both designs have been well researched and documented in the literature.

An experimental study compared the mixing performance of an ET screw, hereafter be referred to as the mixing screw, with a conventional metering screw (11). Mixing performance was assessed from extrudate samples at various letdown ratios of white to black pellets and from extrusion solidification experiments. Axial pressures, rates, discharge temperatures, and energy usage demonstrated that the mixing screw did not adversely affect process performance. In fact, the mixing screw generated pressure, had higher rates, had lower extrudate temperatures, and required less motor energy as compared to the conventional screw.

A new screw design, the VBET screw, seeks to combine the mixing performance of the mixing screw, with improved melting performance (12). This screw will hereafter be referred to as the VB mixing screw. Initial evaluation of the VB mixing screw indicates that maximizing conductive melting as the primary melting mechanism improves the melt quality at high rates. An additional advantage of a conductive melting mechanism is that a more uniform melt temperature distribution can be obtained (13).

This investigation seeks to further assess the performance of the VB mixing screw. This paper describes results from experiments conducted for a VB mixing screw and a mixing screw with an ET mixing section.

Experimental

A highly instrumented, 63.5 mm diameter extruder with a 21 length-to-diameter ratio (L/D) was used to collect extrusion process data. This extruder had eleven pressure transducers along the axis of the barrel to measure pressures along the screw, and it was equipped with three barrel temperature control zones. The pressure transducers were connected to a data acquisition system, which allows pressure data to be collected (14). The extrudate flowed from the extruder through a restrictor valve that was either fully open or partially closed. A hand-held thermocouple was used to measure extrudate temperature.

The mixing screw had a lead-length of 76.2 mm and a primary flight clearance of 0.08 mm. It had an 8-diameter feed section that was 10.9 mm deep, a 6-diameter transition section, and a 7-diameter mixing section. The feed and transition sections were single-flighted, and the mixing section, shown in Figure 1, was designed with two channels. The channel depths were 3.18 mm at the entrance and exit of the mixing section, and within the mixing section they oscillated between 1.45 mm and 6.35 mm, as shown in Figure 2. The period of these oscillations was out of phase for the two channels. In addition, the flights between the channels were undercut to 1.40 mm deep at strategic locations so that flow could occur between the channels. The specific drag flow rate, that is the specific rate expected for just rotation with no imposed pressure gradients, was calculated at 1.0 kg/(h rpm).

The VB mixing screw had a lead-length of 76.2 mm and a primary flight clearance of 0.08 mm. It had a single-flighted feed section that was 5-diameters long and 10.9 mm deep. The transition section was 5-diameters long, with a starting depth of 10.9 mm and end depth of 3.18 mm. Next, the mixing section was 11-diameters long. The channel depths were 3.18 mm at the entrance and exit of the mixing section. Within the mixing section the channel depths were varied between 1.02 mm and 6.35 mm. The channel depths are shown in Figure 3. As with the mixing screw, the period of these oscillations was out of phase for the two channels. However, unlike the mixing screw, the undercut clearance was gradually decreased from 2.3 mm at the entrance of the mixing section to 1 mm at the discharge end of the screw. The specific drag flow rate was calculated at 1.0 kg/(h rpm) for the VB mixing screw, which was the same as the mixing screw.

There are several key differences between the mixing screw and the VB mixing screw. First, the feed and transition sections of the VB mixing screw were 10 diameters, versus 14 diameters for the mixing screw. These sections were shortened on the VB mixing screw to accommodate a longer mixing section. The length of the mixing section on the VB mixing screw was 11 diameters long, versus 7 diameter on the mixing screw. Increasing the length of the mixing section on the VB mixing screw allowed the inclusion of 5 cycles in the mixing section. Also, the undercut clearance was gradually decreased from 2.3 mm at the entrance of the mixing section to 1 mm at the discharge end of the screw. The mixing section of the mixing screw had 3 cycles, and the undercut clearance was a constant 1.40 mm.

The material used for this study was an ABS resin with a melt flow rate of 3.5g/10 min (230°C, 3.8 kg). The white and black ABS pellets contained 2% TiO_2 and 30% pigment concentrate, respectively. The black pellets were designed for a letdown ratio of 35:1. The actual letdown ratios ranged from 100 to 220:1. To investigate the melting and mixing behavior of the two screws, the ABS resin was run on the extruder. The barrel temperatures were set at 200, 230, and 250°C for zones 1 (feed), 2, and 3, respectively. Experiments were conducted with screw speeds that ranged from 30 to 150 rpm.

Results

First, experiments were performed to characterize the mixing performance of the two screws. The extruder was operated with a 100:1 letdown ratio of white pigmented ABS to the black color ABS concentrate pellets. Extrusion rates were measured and samples of the extrudate were collected at 30, 60, 90, 120 and 150 rpm for each screw. These samples were visually examined for mixing. The location for these visual cross-sections is shown by Figure 4. The restrictor valve was fully opened to minimize mixing from high discharge pressures. The high (non-commercial) letdown ratio and low discharge pressure created a very difficult mixing operation.

Cross-sectional slices of the extrudate strand samples for the mixing screw are shown in Figure 5. The white spiral patterns indicate regions where little to no mixing occurred between the white and black resins. These spiral patterns were caused by the flow of the resin over the screw tip. These regions could cause streaking in sheet production for extrusion operations or poor part coloration for injection molding. At a screw speed of 30 rpm, a few white streaks were evident in the extrudate strand samples, likely due to inadequate mixing at the lower screw speed. When the screw speed was increased to 60 rpm, an extrudate that was free of defects was obtained. The same result was achieved when the screw speed was increased to 90 rpm. As the screw speed was further increased to 120 rpm, subtle spiral patterns became more obvious, and solid resin fragments began to appear in the extrudate strand samples. When the screw speed was increased to 150 rpm, the amount and size of the solid resin fragments in the extrudate increased further, as shown in Figure 5. The measured extrusion rate for the mixing screw is also shown in Figure 5. At a speed of 30 rpm, the specific rate of the mixing screw was 1.10 kg/(h rpm). As the speed increased, the specific rate decreased. For example at 90 rpm, the specific rate was 0.94 kg/(h rpm), and decreased further to 0.90 kg/(h rpm) at 150 rpm. This decrease in specific rate with increasing screw speed is typical for flood-fed extruders.

Cross-sectional slices of the extrudate strand samples for the VB mixing screw are shown in Figure 6. As before, the white spiral patterns indicate regions where little to no mixing occurred between the white and black resins. At a screw speed of 30 rpm, very few white streaks were evident in the extrudate strand samples. When the screw speed was increased to 60 and 90 rpm, the extrudate changed little. As the screw speed was further increased to 120 rpm, the spiral patterns became more obvious, however, there were no solid resin fragments in the extrudate samples; some solid fragments were evident for the mixing screw at this speed. When the screw speed was increased to 150 rpm, a few solid resin fragments in the extrudate began to appear as shown in Figure 6. The measured extrusion rate for the VB mixing screw is also shown in Figure 6. At a speed of 30 rpm, the specific rate of the VB mixing screw was 1.00 kg/(h rpm). As the speed increased, the specific rate remained essentially the same. For example at 90 rpm, the specific rate was also 1.00 kg/(h rpm), and decreased only slightly to 0.99 kg/(h rpm) at 150 rpm. These results indicate that the VB mixing screw has improved melting capacity, as there were fewer unmelted pellets in the extruder discharge at higher screw speeds and higher specific rates.

Next, the performances of the screws were evaluated more closely under one set of operating conditions. The results of the extrusion trials where both screws were operated at 60 rpm are summarized in Table 1. The specific rates for the mixing screw was slightly higher than that for the VB mixing screw. The discharge pressure was 9.5 MPa for the mixing screw, and 8.6 MPa for the VB mixing screw. This difference in discharge pressure may be due to the slightly higher rate and lower discharge temperature for the mixing screw. The discharge temperature of the ABS resin was 254°C for the mixing screw, and it was 258°C for the VB mixing screw. The specific energies inputted by the screws were 480 and 496 J/g for the mixing and VB mixing screws, respectively. In both cases, the extrudate quality was good; i.e., no unmelted particulates in the extrudate and stable rates.

The pressure profiles along the barrel for both screws operating at 60 rpm are shown in Figure 7. The pressures in the feed and transition sections were very different for the two screws. The pressure for the mixing screw was approximately 5 MPa at the entrance of the transition section at 7 diameters. The pressure increased to a maximum of 16 MPa at 12 diameters, then decreased to 9 MPa at the start of the mixing section at 14 diameters. The pressure for the mixing screw reached a minimum at the entrance to the mixing section, indicating decreased resistance to flow as one of the mixing channels began to deepen. After this, the pressure increased, demonstrating the mixing section could drive flow and generate pressure.

The pressure for the VB mixing screw was approximately 2 MPa at 7 diameters, which was nearly one-third of the length of the transition section. Then the pressure increased to 3.5 MPa between 8 and 13 diameters. The pressure then increased from 3.5 MPa at 13 diameters to around 11 MPa at the end of the screw.

Next, the melting and mixing performance were evaluated through screw solidification experiments (1, 2). Each screw was run at 60 rpm at the previously mentioned process conditions until steady-state operation had been achieved. The rotation of the screw was then abruptly stopped, and the barrel was rapidly cooled, solidifying the polymer in the screw channels. The screw was extracted and the helical channel was cut lengthwise along a plane running parallel to the screw axis, revealing the screw channel cross-section. Figures 8 and 9 show these cross sections at axial distances of 6 to 21 diameters from the feed throat. Like the extrudate samples, the white regions indicate poor mixing because the white resin had not yet melted or the melted resin was not adequately mixed with the black concentrate. Because the black color concentrate was such an effective colorant, dark gray areas indicate where the white and black pellets melted, came in contact, and were well mixed.

As shown in Figures 8 and 9, the cross-sectional slices at axial distances less than 10 diameters were similar for both screws. For example, the slices at 6 diameters were comprised of a compacted bed of discrete pellets. The slices at 8.4 diameters were in the transition section, where the pellets compacted, softened and began to melt. For the mixing screw, the compaction process had just begun at 8.4 diameters, which was only 0.4 diameters into the transition section, so discrete pellets (one black) were still visible. For the VB mixing screw, melting was further along at 8.4 diameters, which was 3.4 diameters into the transition section. Fewer individual pellets were distinguishable and the melt pool was more mixed with finer circular striations.

At axial distances of 10 diameters and greater, the slices were different, as the mixing section on the VB mixing screw started at this point, while the mixing section for the mixing screw started at 14 diameters. The slice at 10.2 diameters for the VB mixing screw in Figure 9 shows that individual pellets were no longer distinguishable and the melt pool had increased in width. This slice was also at the start of the secondary flight, which can be seen as a depression on the middle of the lower edge of the slice. From this point forward, the secondary flight started and separated the channel into the A and B channels, as indicated in Figure 9. At 11.4

diameters, the B-channel depth decreased and displaced molten resin and solid bed material into the A-channel, as can be seen from the white and dark regions in the slice. As the solid bed and melt advanced to 12.6 diameters, the material flowed over the secondary flight into the B-channel. The white domains are regions of the broken up solid bed that are surrounded by regions of black molten resin. Next, the resin was transferred to the B-channel by decreasing the A-channel height and allowing the material to flow over the undercut between the channels. The material at 13.2 diameters is comprised of a mix of solid white material surrounded by molten black resin, but fewer solids are visible at this point than earlier. At 15 diameters, the two channels are shown connected by the undercut between the channels. Oscillation of material continued between the A and B channels as shown in Figure 9. By the end of the screw, the solids had been melted and the white resin and black concentrate had been well mixed, as shown by the slice at 21 diameters for the VB mixing screw.

The transition section in the mixing screw continued up to 14 diameters. The slice at 12 diameters in Figure 8 shows that the melt pool continued to increase, and that the solid bed was fully compacted. At 14.4 diameters, the secondary flight on the mixing screw started, dividing the slice into two channels connected by an undercut flight. This slice was only 0.4 diameters into the mixing section; so much of the resin was still only softened, with the most of the gray molten resin segregated to the melt pool. The mixing screw slice at 15.6 diameters had a segregated gray melt pool in the A-channel and much of the B-channel encompassed by white resin, similar to the slice at 14.4 diameters. For this slice, the B-channel was shallow, so the resin experienced additional shear heating as white resin in the B-channel was displaced over the flight undercut and into the adjoining and deeper A-channel. At 17.4 diameters, the flight undercut reappeared and connected the now shallow A-channel to the upstream, and deepening, B-channel. Because the A-channel was shallow at 17.4 diameters, many of the remaining fragments of white resin were trapped, shear-heated and melted there. Furthermore, the undercut allowed resin to flow into the upstream B-channel, where resin-to-resin heat transfer and mixing occurred. The flight undercut then disappeared at 18 diameters. These trends continued at downstream positions, and the unmixed fragments of white resin becoming smaller due to periodic high shear balanced by resin-to-resin heat transfer and mixing. Finally, at the end of the screw, or 21 diameters shown in Figure 8, the material appeared to be molten and well mixed.

Discussion

The data presented here clearly show the advanced melting and mixing capability of the VB mixing screw. As shown by the extrudate samples, the VB mixing screw can be designed to allow higher screw speeds and rates before solids are discharged in the extrudate. For the cases presented here, the mixing screw can be operated at a maximum rate of about 85 kg/h (90 rpm) while the VB mixing screw can run at about 121 kg/h (120 rpm). Thus, the maximum rate for the VB mixing screw is about 40% higher than that for the mixing screw, while maintaining high melt quality.

The solidification experiments indicate that the resin melts earlier for the VB mixing screw. This start of early melting combined with the decreasing clearance of the undercut permit the VB mixing screw to outperform the mixing screw design.

Conclusions

Extrudate discharge sampling combined with the screw solidification experiments clearly show the performance advantages of a VB mixing screw. For the design studied here, the maximum rate of the extruder is about 40% higher for the VB mixing screw as compared to the mixing screw, while also providing a high quality discharge at low and acceptable discharge temperatures.

References

1. C.I. Chung, *Extrusion of Polymers: Theory and Practice*, Hanser, Munich (2000).
2. B.H. Maddock, *SPE J.*, **15**, 383 (1959).
3. B.H. Maddock, *SPE J.*, **23**, 23 (1967).
4. G.A. Kruder and W.N Calland, *SPE ANTEC Tech. Papers*, **36,** 74 (1990).
5. G.A. Kruder, U.S. Patent 4,173,417 (1979).
6. C.I. Chung and R.A. Barr, *SPE ANTEC Tech. Papers*, **29**, 168 (1983).
7. C.I. Chung and R.A. Barr, U.S. Patent 4,405,239 (1983).
8. T.A. Plumley, M.A. Spalding, J. Dooley, and K.S. Hyun, *SPE ANTEC Tech. Papers*, **40**, 324 (1994).
9. S.A. Somers, M.A. Spalding, J. Dooley, and K.S. Hyun, *SPE ANTEC Tech. Papers*, **41,** 222, (1995).
10. B.A. Salamon, M.A. Spalding, J.R. Powers, M. Serrano, W.C. Sumner, S.A. Somers, and R.B. Peters, R.B., *Plast. Eng.*, **57**, 4, 52 (2001).
11. S.A. Somers, M.A. Spalding, J. Dooley, and K.S. Hyun, *SPE ANTEC Tech. Papers*, **48**, 307 (2002).
12. R.A. Barr, U.S. Patent Pending (2001).
13. J.A. Myers and R.A. Barr, *SPE ANTEC Tech. Papers*, **48**, 154 (2002).
14. M.A. Spalding, J. Dooley, K.S. Hyun, and S.R. Strand, *SPE ANTEC Tech. Papers,* **39**, 1533 (1993).

Key Words

Screw Design, ET, Melting, Mixing, ABS

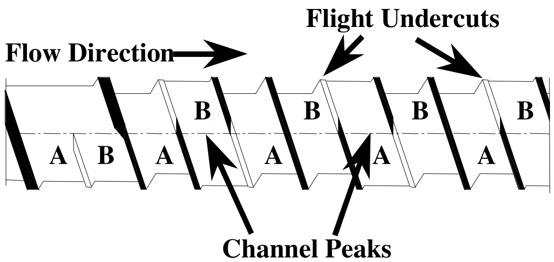

Figure 1. Channel Depth Profile for the Mixing Screw.

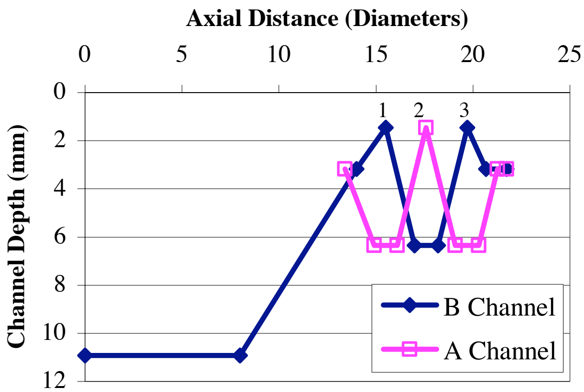

Figure 2. Channel Depth Profile - Mixing Screw.

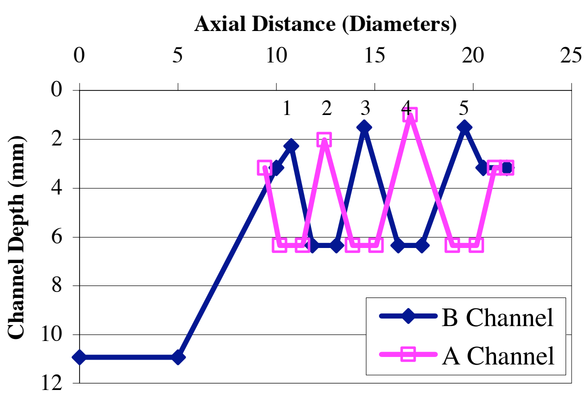

Figure 3. Channel Depth Profile - VB Mixing Screw.

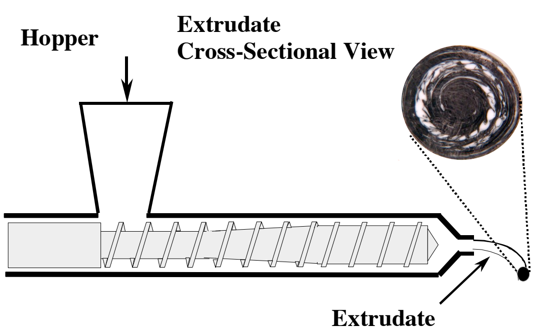

Figure 4. Extruder Schematic Showing Location of the Extrudate Cross-sectional Views.

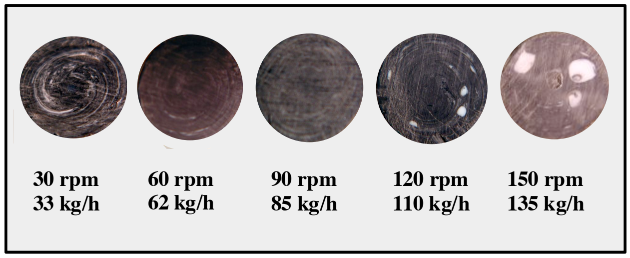

Figure 5. Cross-sectional Slices of Extrudate Samples and Extrusion Rates at 5 Screw Speeds for the Mixing Screw.

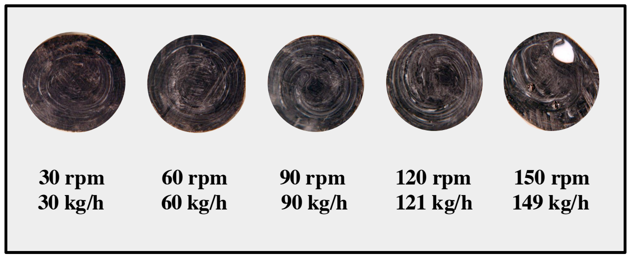

Figure 6. Cross-sectional Slices of Extrudate Samples and Extrusion Rates at 5 Screw Speeds for the VB Mixing Screw.

Table 1. Extrusion Results for the Mixing and VB Mixing Screws at 60 rpm.

Screw	Mixing Screw	VB mixing Screw
Rate, kg/h	62	60
Specific Rate, kg/(h rpm)	1.03	1.00
Average Discharge Pressure, MPa	9.5	8.6
Average Discharge Temperature, °C	254	258
Specific Energy, J/g	480	496

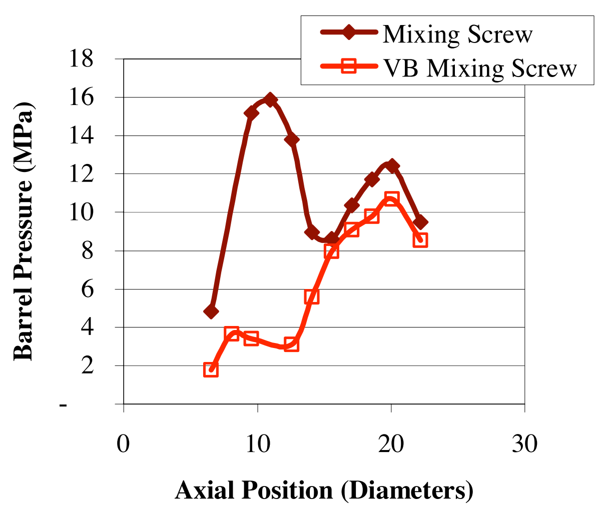

Figure 7. Pressure Profile at 60 rpm.

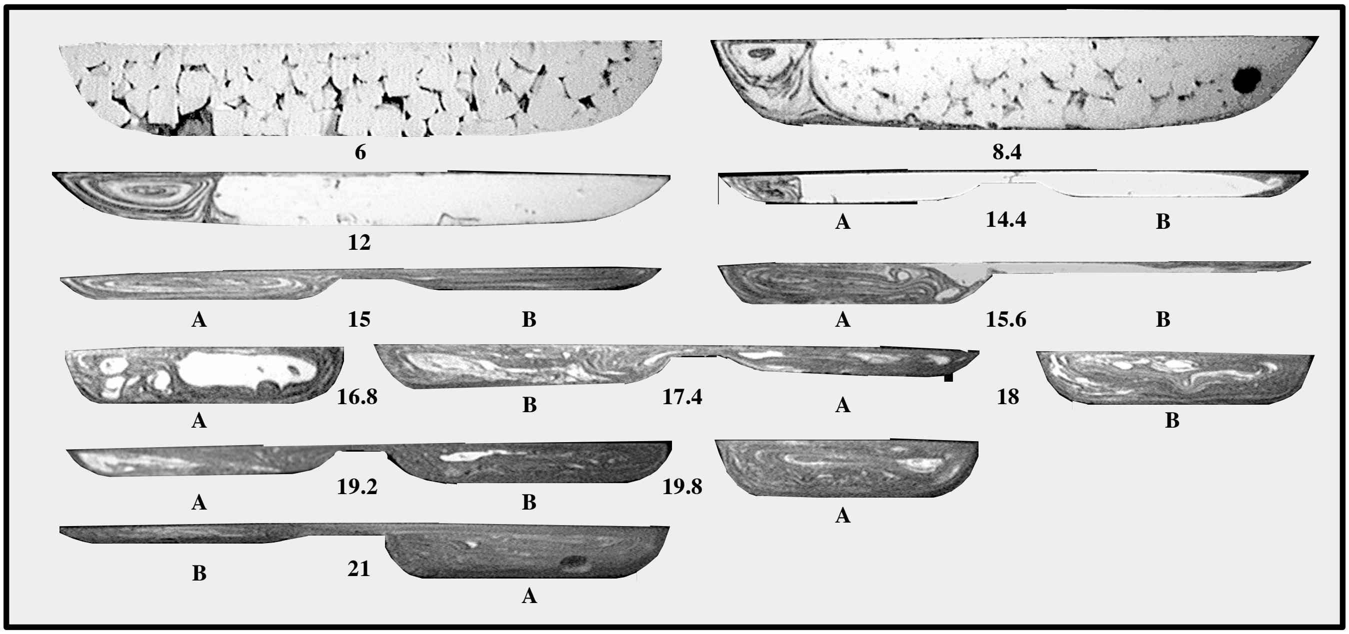

Figure 8. Screw Heel Samples for the Mixing Screw.

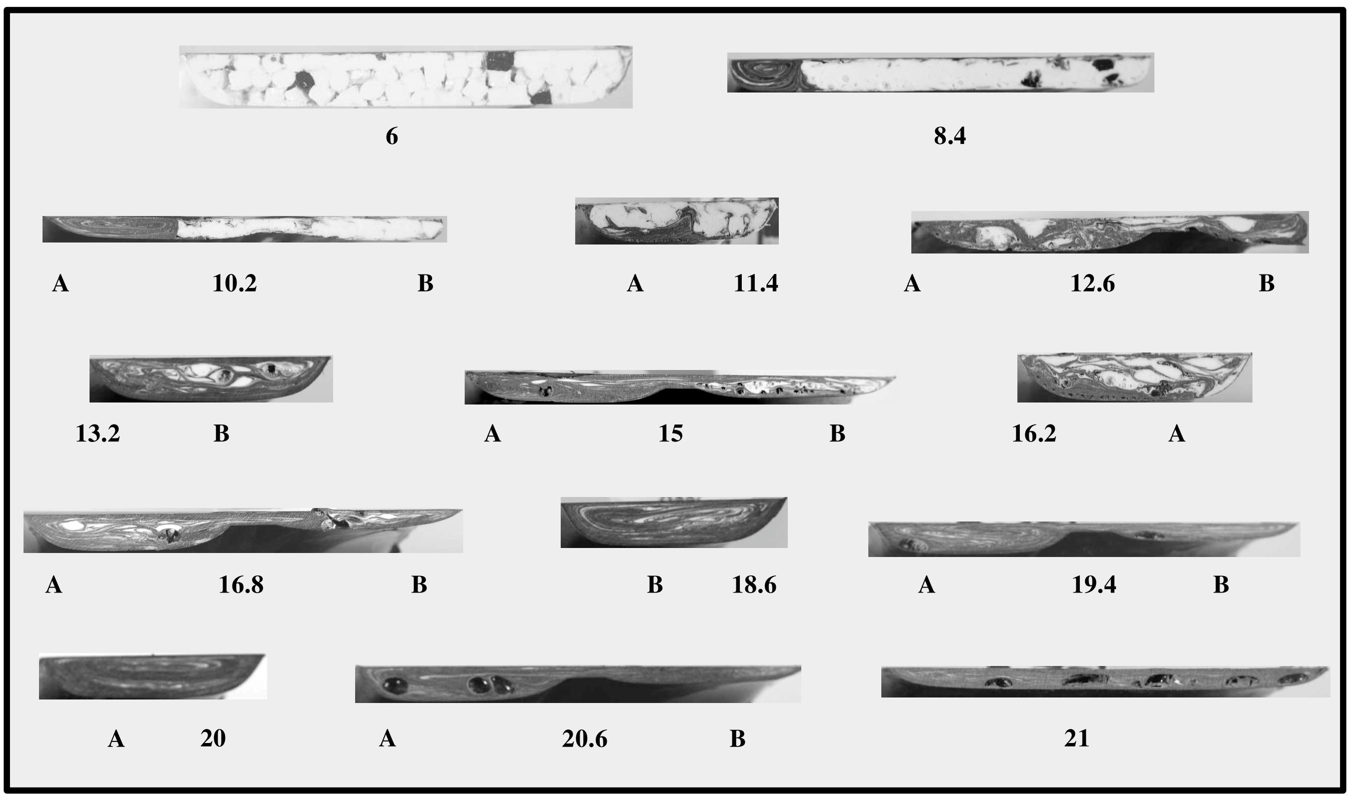

Figure 9. Screw Heel Samples for the VB Mixing Screw.